Paper No.
06372

CORROSION
NACExpo 2006
61ST ANNUAL CONFERENCE & EXPOSITION

GENERAL CO_2 CORROSION IN HIGH SALINITY BRINES

Haitao Fang, Srdjan Nesic, Bruce Brown
Institute for Corrosion and Multiphase Technology
342 West State Street
Ohio University, Athens, Ohio 45701, USA

Shihuai Wang
Champion Technologies
3130 FM 521
Fresno, TX 77545

ABSTRACT

The general CO_2 corrosion rates of C1018 carbon steel have been measured for NaCl concentrations 3 – 25 wt% at 5ºC, pH4.0. The corrosion process was monitored by linear polarization resistance and potentiodynamic sweeps. Experimental results show that high salt concentrations affect the general CO_2 corrosion rate significantly and nonlinearly. Potentiodynamic sweep analysis shows that the high content of salt retards both cathodic and anodic process. No significant effects of velocity on corrosion rates are seen for various saline conditions

Keywords: CO_2 corrosion, carbon steel, linear polarization resistance, potentiodynamic sweep, high salt concentration.

INTRODUCTION

Carbon dioxide (CO_2) saturated aqueous system is one of the most common corrosive environments encountered in the oil and gas industry. A large body of research has been conducted in this field over the last three decades. The first significant CO_2 corrosion model, introduced by deWaard and Milliams in 1975, identified the combined effect of CO_2 partial pressure and temperature on the corrosion rate[1] as the key parameters in CO_2 corrosion. Since then many other parameters have been uncovered such as pH, velocity, etc.[2, 3, 4] However, CO_2 corrosion in solutions with high salt concentrations, i.e. in solution with high ionic strength, or non-ideal solution, has not been addressed properly.

Previous research related to the effect of salt on CO_2 corrosion focused on the effect of chloride ion concentration in localized corrosion. Sun investigated the effect of Cl^- on localized corrosion in wet gas pipelines[5]; Ma also studied the influence of chloride ions on the corrosion of iron[6]. Both investigations concluded that chlorides accelerate localized corrosion. However, the effect of salt content on general CO_2 corrosion was not even mentioned in either paper.

Salt content of formation water varies dependent upon the location. Water analysis from a Texas gas well is shown in Table 1. Salt content is about 23% by weight and is not considered to be an isolated case. It is not uncommon that salt crystals are seen in the production tubing in Texas, meaning salt concentration could be near saturation. So it is important to know if this high content of salt has effects on CO_2 corrosion or not.

Most CO_2 corrosion research is done at lower salt concentrations typically from 1 wt% to 3 wt% NaCl. No significant effects of salt concentration on general CO_2 corrosion are observed in this range. It was therefore commonly assumed that general CO_2 corrosion of bare steel is not effected by salt concentration. However, this hypothesis is based on the data obtained at relatively low salt concentration. No published information about CO_2 corrosion in solution with high salt concentration (>3 wt%) can be found, and the present study aimed at filling this gap by performing general CO_2 corrosion experiments in brines containing up to 25 wt% NaCl which is close to the solubility limit. It should be noted that effects of salt on protective film formation and localized corrosion are not included here, and that they are the subject of ongoing work and will be reported in subsequent publications.

EXPERIMENTAL PROCEDURE

Glass Cell

A picture of the test cell is shown in Figure 1. A three-electrode system was used with the counter electrode made of platinum, the saturated Ag/AgCl reference electrode connected externally to the cell via a Luggin capillary tube through a porous Vicor tip and a working electrode in the form of a rotating cylinder made of C1018 steel. A gas bubbler within the test cell solution was used for purging and to assure a positive pressure of carbon dioxide in the test cell and reduce the chance of oxygen contamination.

Specimen Preparation

One type of carbon steel (C1018) is used for the LPR and potential dynamic sweep analysis. The exposed surface area of the specimen is 5.4cm^2. The chemical composition of the carbon steel used in the test is shown in Table 2.

The specimen was polished by silicon carbide sand paper before it was tested, and the sand paper was used in the following order: 240, 400, 600 grit. After polishing, the specimen was immersed in isopropyl alcohol contained in an ultrasonic cleaner for 1 to 2 minutes and then air dried.

pH Measurement

The determination of the correct pH value in high saline solutions is an important issue during corrosion studies. Theoretically, an increase in salt concentration will cause the pH to increase because more salt is dissolved in the solution, which means less CO_2 can be dissolved in the solution and less carbonic acid is formed. But, in reality, the measured pH in high salt concentration solutions was lower than the measured pH in low salt concentration solutions. A water chemistry model[7] based on Pitzer's theory, was used to calculate the activity coefficient of each ionic species in solution at different salt concentrations and also to predict the pH. Figure 2 shows the activity coefficient changes for deoxygenated saline solutions at 1 bar total pressure, purged with carbon dioxide. The most notable observation is that the salt concentration has a big effect on the activity coefficient of the H^+ ion. In a 20 wt% NaCl solution, the activity coefficient for H^+ ion is 3 times greater than it is in a solution with 3 wt% NaCl and is 5 times greater in a 25 wt% NaCl. Figure 3 shows the comparison of measured pH value and predicted pH value. Experiment results show some deviation between the measured pH value and predicted pH value, which is more significant at high salt concentrations. Overall, it was concluded that the decrease in pH is due to change of the activity of the H^+ ion and that the measured value is accurate enough for the purposes of the subsequent corrosion measurements.

In order to clarify the salt effect on the CO_2 corrosion rate, only the concentration of NaCl in solution was varied while the pH was held constant. However, as shown above, the change in the salt content also changes the pH. Therefore before beginning each corrosion experiment, the pH value was measured and adjusted to the desired pH which was 4.0 in this study.

Corrosion Measurement

The experimental apparatus, Figure 1, was set up inside a refrigerator to reach the desired temperature of 5^{o}C. Carbon dioxide was bubbled to de-oxygenate the solution. When the working temperature was reached, the pH of the test solution was adjusted by adding de-oxygenated sodium bi-carbonate solution. Once the solution was fully prepared, the polished working electrode inserted into the solution and all electrical connections made. The rotational speed was immediately set, and 40 to 60 minutes waiting was required to have the open circuit potential (OCP) stabilize within $\pm$ 1 mV so that reliable electrochemical measurements could be made.

The test matrix for this experimental series is shown in Table 3. The LPR measurement was conducted by polarizing ±10 mV around the corrosion potential and scanning at 0.125 mV/s. Solution resistance was measured using alternating current (AC) impedance at each test conditions and was considered to be negligible in each case.

After determining the corrosion rate by LPR method, the potentiodynamic sweep was conducted, starting 550mv below and finishing 150mv over the open circuit potential with scan rate of 0.2mv/s to obtain both the cathodic and anodic characteristics.

RESULTS

More than 20 glass cell experiments have been conducted. Some of the tests were repeated to several times to check the reproducibility of the results. Based on previous studies, the Tafel slopes used in the LPR corrosion rate were calculated for the test temperature according to:

$$\beta_c = \frac{2.3RT}{\alpha nF} = 112 \text{ mV} \quad (1)$$

$$\beta_a = \frac{2.3RT}{(1-\alpha)nF} = 37 \text{ mV} \quad (2)$$

Three repeated sets of experiments were conducted at each of the four salt concentrations. Each experiment was conducted at a fixed pH4.0 and 5°C while the rotational speed was varied from 100 rpm to 6000 rpm to observe the flow velocity effect on the corrosion process.

Tests with 3wt% NaCl

Figure 4 shows the corrosion rate results measured by LPR at the different rotational speeds for 3 wt% NaCl solution. The LPR corrosion rate is approximately 0.25-0.3 mm/yr over the whole range of velocities. i.e. the corrosion process is velocity insensitive for these conditions. Figure 5 shows the potentiodynamic sweep results at different flow velocities. The cathodic limiting current is flow sensitive what is consistent with a mixed mass transfer / chemical reaction mechanism typical for CO_2 corrosion at pH4.0. Interestingly, a very clear straight line section of the cathodic curve can be seen at higher velocity, what is reminiscent of a Tafel behavior, however, the apparent 200 mV slope is difficult to justify from a theoretical point of view. This subject is under investigation. Even if the flow velocity had an effect on the cathodic limiting current, the corrosion rates did not depend on flow clearly suggesting that the corrosion process is under charge transfer control what was confirmed by the sweeps: the corrosion current is at least one order of magnitude lower then the limiting current. The clarity of the data along with the reproducibility obtained at this temperature was the reason that the subsequent experiments with high salt concentration were done at 5°C as well.

Tests with 10wt% NaCl

The LPR corrosion rate results for 10wt% NaCl solution are shown in Figure 6. The LPR corrosion rate is approximately 0.1 mm/y which is 2-3 times lower then at 3 wt% salt. Clearly there is a significant retardation effect of NaCl on the corrosion rate. The corrosion rate at 10 wt% shows no flow sensitivity. In Figure 7 the potentiodynamic sweep results at different rotational speeds are displayed. The cathodic limiting currents did not change from 100 rpm to 1000 rpm but then increased significantly

for 6000 rpm. On the other hand, the anodic portion of the sweep takes on the "usual" appearance at 6000 rpm while at lower velocity there appears to be a retardation effect which vanishes at higher overpotentials and current densities. Just like at 3 %wt, the corrosion current is at least one order of magnitude lower then the limiting current, explaining the lack of flow sensitivity. Both the anodic and cathodic behavior, as well as the retarded corrosion rate, qualitatively suggest that there appears to be "protective" layer of some sort at the steel surface which is rather easily removed by flow or polarization.

Tests with 20wt% NaCl

Figure 8 shows the LPR corrosion rate results for 20 wt% NaCl solution. The average corrosion rate (0.05 mm/yr) is further decreased by a factor 2, compared with the 10 wt% NaCl solutions. Similarly to the previous results, there is no significant flow sensitivity of the corrosion rate. Figure 9 shows the potentiodynamic sweep results. The flow velocity does not appear to affect either the cathodic or the anodic reaction which clearly explains the lack of flow effect on the corrosion rate. The cathodic reaction, while retarded takes on a "typical" appearance, while the anodic reaction indicates inhibition at the corrosion potential, which disappears at higher overpotentials.

Tests with 25wt% NaCl

Figure 10 and Figure 11 show the LPR and potentiodynamic sweep results in a 25 wt% NaCl solution. The results are very similar to those measured in a 20 wt% NaCl solution: retardation of all reactions and lack of flow sensitivity.

DISCUSSION

Figure 12 shows the NaCl concentration effect on the LPR corrosion rates. It is seen that NaCl significantly reduces the CO_2 corrosion rate. Approximately a factor of two reduction is seen between 3 and 10 wt% NaCl, and then another factor of two between 10 and 20 wt% NaCl. No further decrease in corrosion rate could be measured as the NaCl concentration is increased from 20 wt% to 25 wt%.

The potentiodynamic sweeps are consistent with the corrosion measurements. In Figure 13, Figure 14 and Figure 15 the sweeps are shown as a function of salt concentration. In all three plots (displaying three different velocities) it is obvious that salt retards both the cathodic and anodic reaction. For the cathodic reaction the presence of salt decreases the magnitude of the charge transfer reactions (as indicated by the linear sloped portions of the curves) as well as the limiting current which is under mixed mass transfer-chemical reaction control (denoted by the more vertical portions of the curves). On the anodic side, there seems to be a clear retardation of the rate of anodic dissolution of iron which leads to an increase of the corrosion potential. This effect seems to vanish as the anodic overpotential and current density increase. i.e. as the steel surface is forced to corrode faster, when all the curves come closer together. This behavior is frequently seen with corrosion inhibitors, however typically much larger overpotentials are required to cause the same effect.

The nature of the retardation shown in Figure 12 appears to be consistent with an adsorption controlled mechanism, which is corroborated by the appearance of the potentiodynamic sweeps, however, a more detailed analysis and modeling of the salt effect is the subject of an ongoing effort.

CONCLUSIONS

- General CO_2 corrosion rate decreases strongly and non-linearly with an increase in NaCl concentration at 5 ºC, pH4.0.
- An increase in salt concentration retards both the cathodic and the anodic corrosion processes.
- No significant effects of velocity on corrosion rates are seen for various saline conditions tested in a pH4.0 solution at 5 ºC.

REFERENCES

1. C.de Waard, U.Lotz, "Prediction of CO_2 Corrosion of Carbon Steel," Corrosion/93, Paper no. 69, NACE International, Houston, Texas, 1993.

2. C.de Waard, U.Lotz, A.Dugstad "Influence of Liquid Flow Velocity on CO_2 Corrosion: A Semi-empirical Model". Corrosion/95, Paper no. 128, NACE International, Houston, Texas, 1995.

3. B.F.M.Pots "Mechnistic models for the prediction of CO_2 corrosion rates under multi-phase flow conditions". Corrosion/95. Paper no. 137, NACE International, Houston, Texas, 1995.

4. S. Nesic, J. Postlethwaite, and S. Olsen "An Electrochemical Model for Prediction of Corrosion of Mild Steel in Aqueous Carbon Dioxide Solutions", Corrosion Science 2003, 52, P.280.

5. Y. Sun, K, Gorge, S, Nesic "The Effect of Cl^- and Acetic Acid on Localized CO_2 Corrosion in Wet Gas Flow", Corrosion/2003. Paper no. 03327, NACE International, Houston, Texas, 2003.

6. H.Y.Ma, C.Yang, G.Y.Li, W.J.Guo, S.H.Chen, J.L.Luo "Influence of nitrate and chloride ions on the corrosion of iron", Corrosion Science 2003, 59, P.1112.

7. ScaleSoftPitzer Version 8.1, Rice University Brine Chemistry Consortium Energy & Environmental Systems Institute Rice University Houston, TX, 77005.

TABLES

Table 1. The result of the water analysis of one gas flow well in Texas

Compound					Compound	X	Y	Compound
	FW	X/X+Y	Y/X+Y	TOTAL	(mg/l)	(mg/l)	(mg/l)	(g)
NaCl	58.44	0.39	0.61	1.00	131080	51566.2	79513.8	496.14
$CaCl_2.2H_2O$	147.02	0.27	0.48	0.75	111510	30399.4	53775.4	422.07
$MgCl_2.6H_2O$	203.33	0.12	0.35	0.47	50810	6074.8	17717.2	192.32
$SrCl_2.6H_2O$	266.64	0.33	0.27	0.59	0	0.0	0.0	0.00
$BaCl_2.2H_2O$	244.28	0.56	0.29	0.85	0	0.0	0.0	0.00
KCl	74.55	0.52	0.48	1.00	0	0.0	0.0	0.00
Na_2SO_4	142.04	0.32	0.68	1.00	0	0.0	0.0	0.00
$NaHCO_3$	84.01	0.27	0.73	1.00	0	0.0	0.0	0.00
$BaSO_4$	233.40	0.59	0.41	1.00	0	0.0	0.0	0.00
H_2O	18.02							

Table 2. Chemical Composition of Type C1018 Carbon Steel (wt.%)

C	Si	P	S	Mn	Al	Fe
0.21	0.38	0.09	0.05	0.05	0.01	balance

Table 3. Test Matrix for Glass Cell Experiments

Parameters	**Conditions**
Total Pressure	1bar
Temperature	5ºC
Rotation Speed	100, 1000, 6000 rpm
Solution	3, 10, 20, 25 wt% NaCl
pH	4.0
Material	C1018

FIGURES

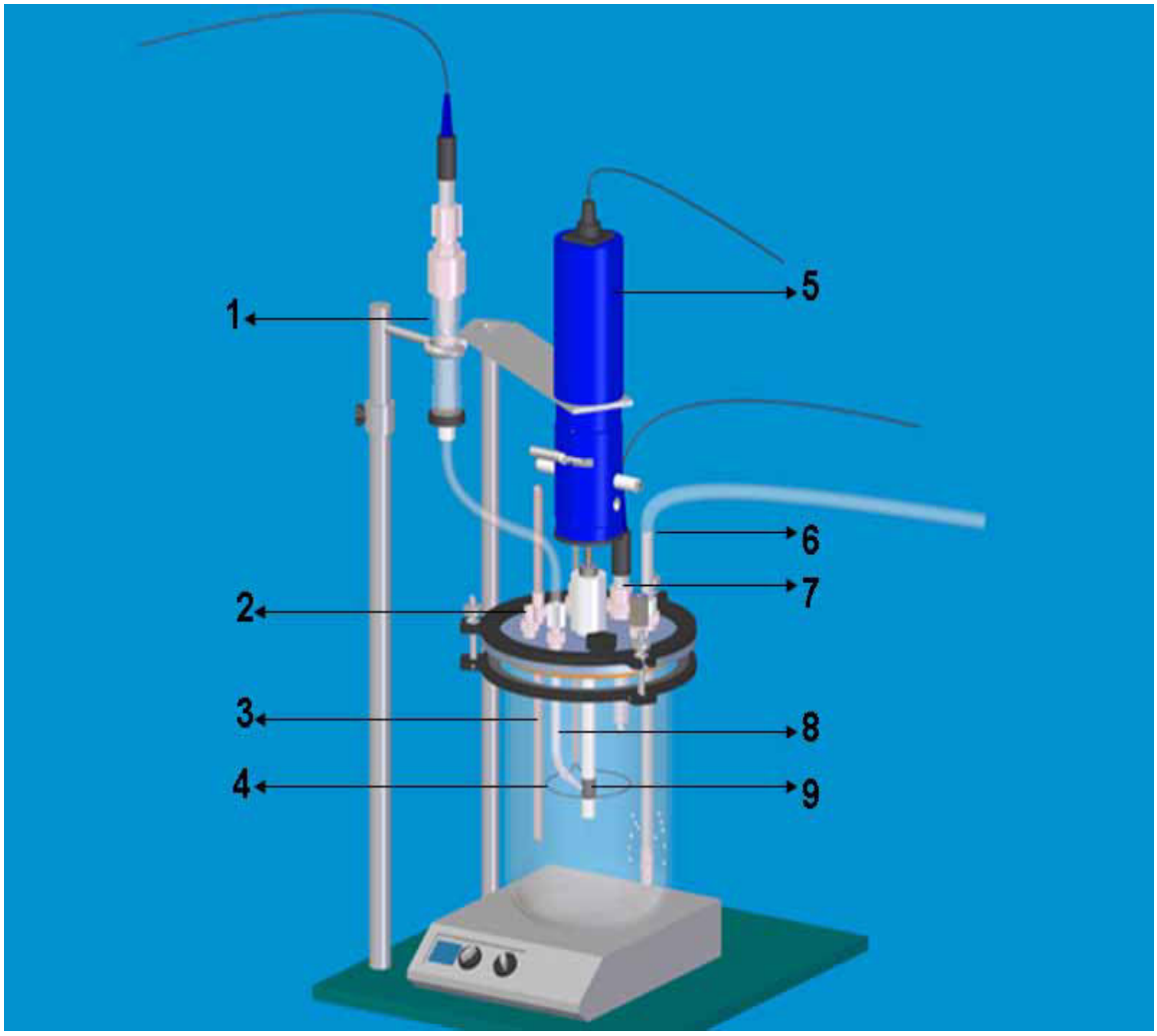

1. Reference electrode
2. Gas outlet
3. Temperature probe
4. Platinum counter electrode
5. Rotater
6. Gas inlet
7. pH-electrode
8. Luggin capillary
9. Working electrode

Figure 1. Glass cell set up

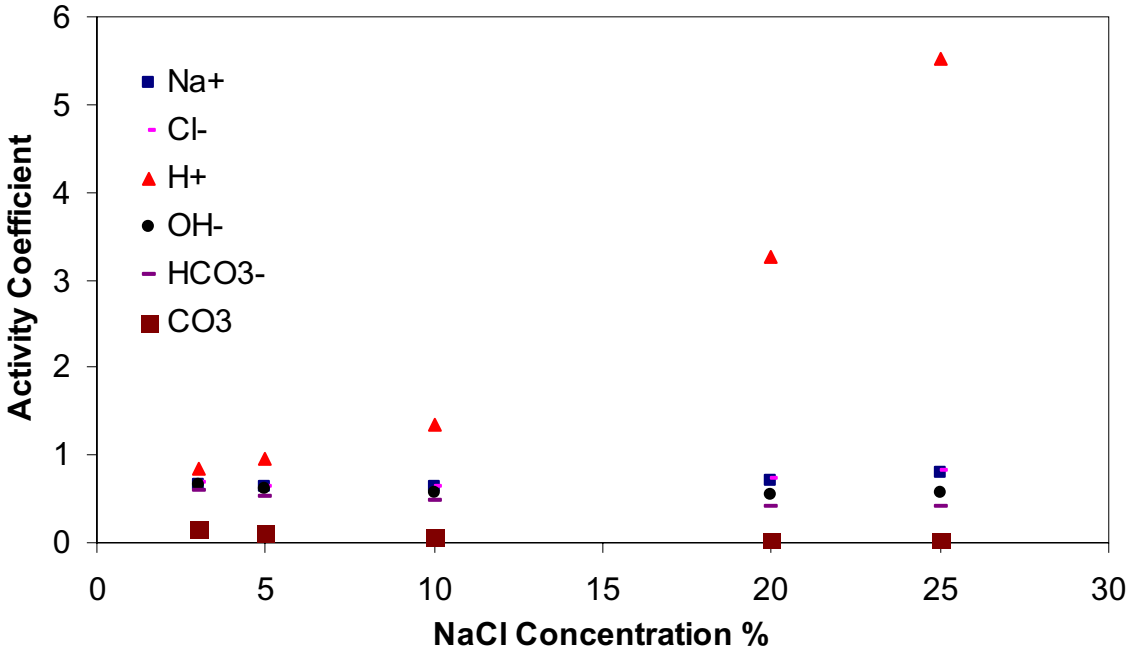

Figure 2. Activity coefficient change with salt concentration at 5ºC for Na^+, Cl^-, H^+, OH^-, HCO_3^- and CO_3^{2-}, at 1 bar total pressure.

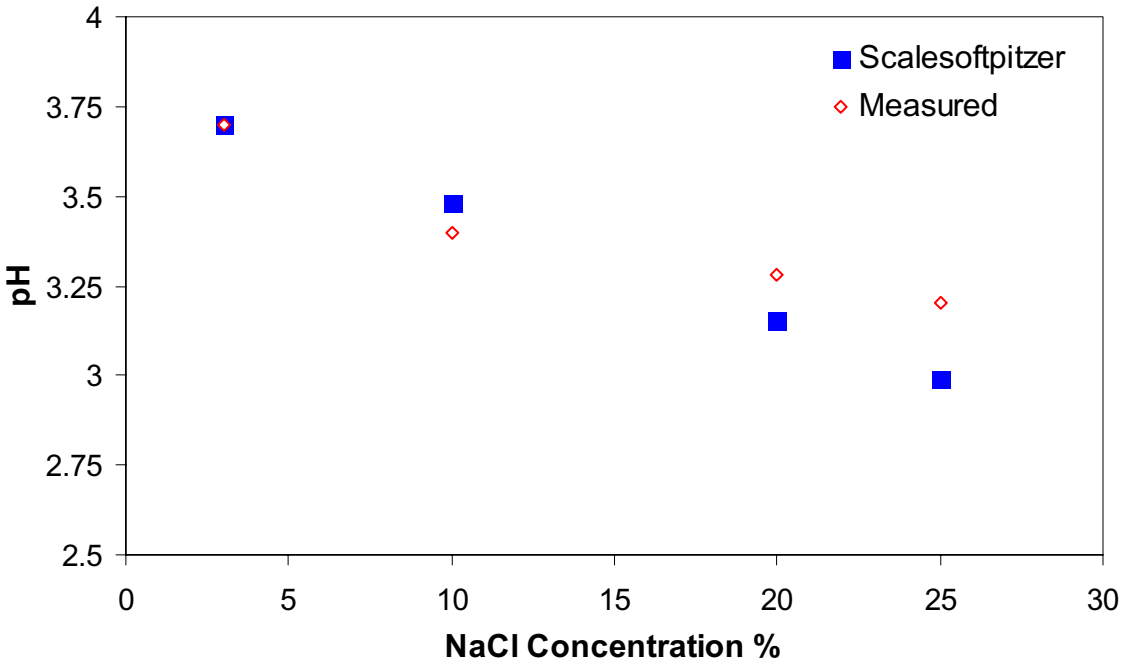

Figure 3. Comparison of measured pH and predicted pH at different salt concentrations at 5 ºC, 1 bar total pressure.

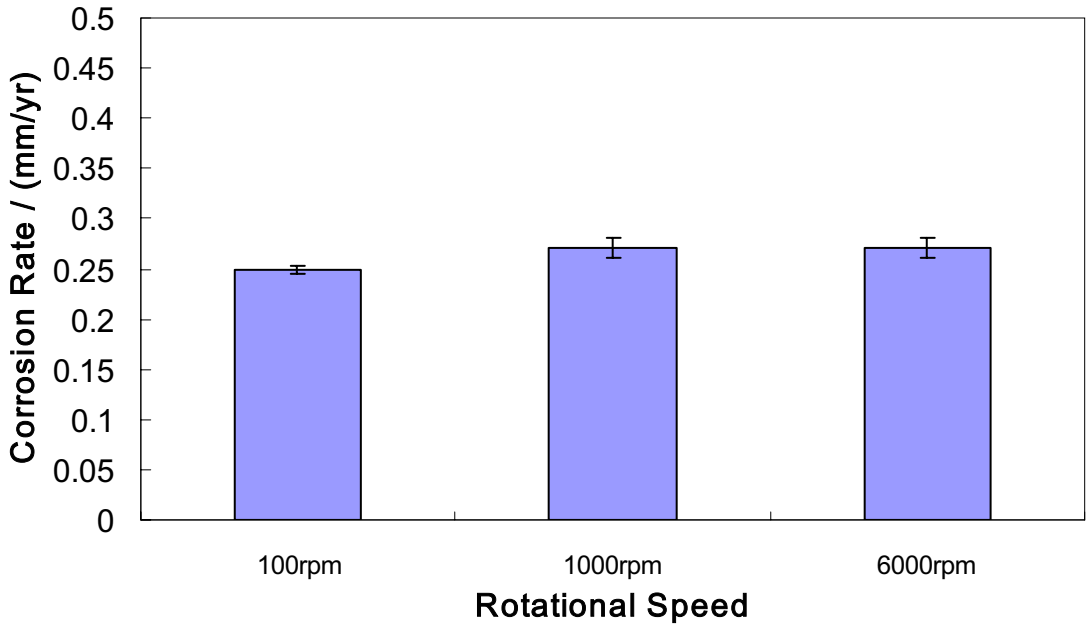

Figure 4. LPR corrosion rates for different rotational speeds at 5 ºC, pH4.0, 3% NaCl

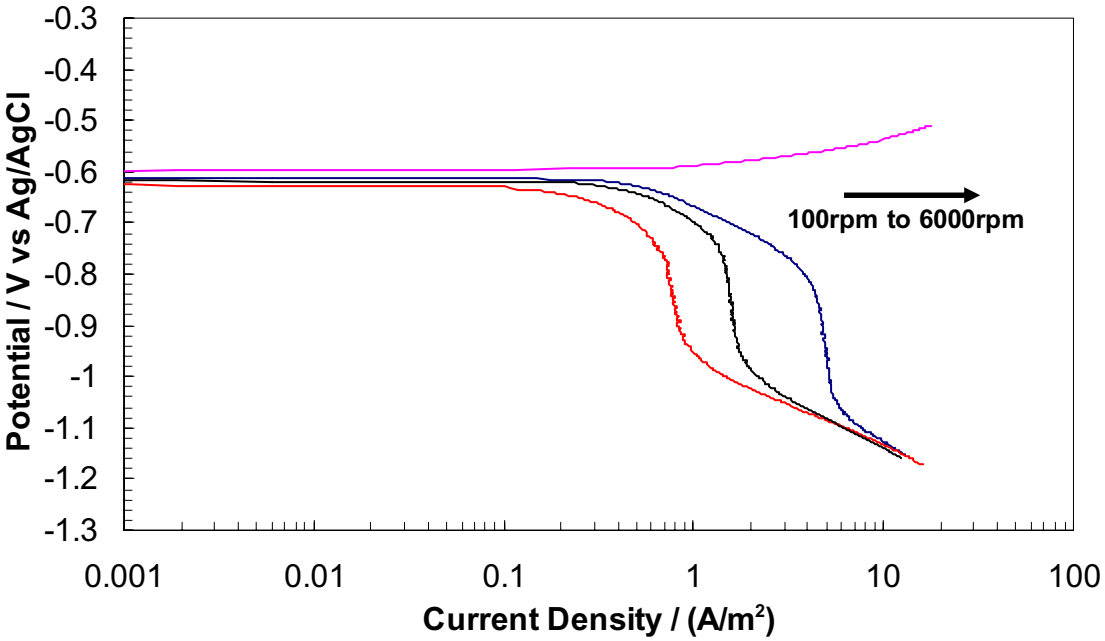

Figure 5. Potentiodynamic sweeps for different rotational speeds (100, 1000, 6000rpm) at 5ºC, pH4.0, 3% NaCl

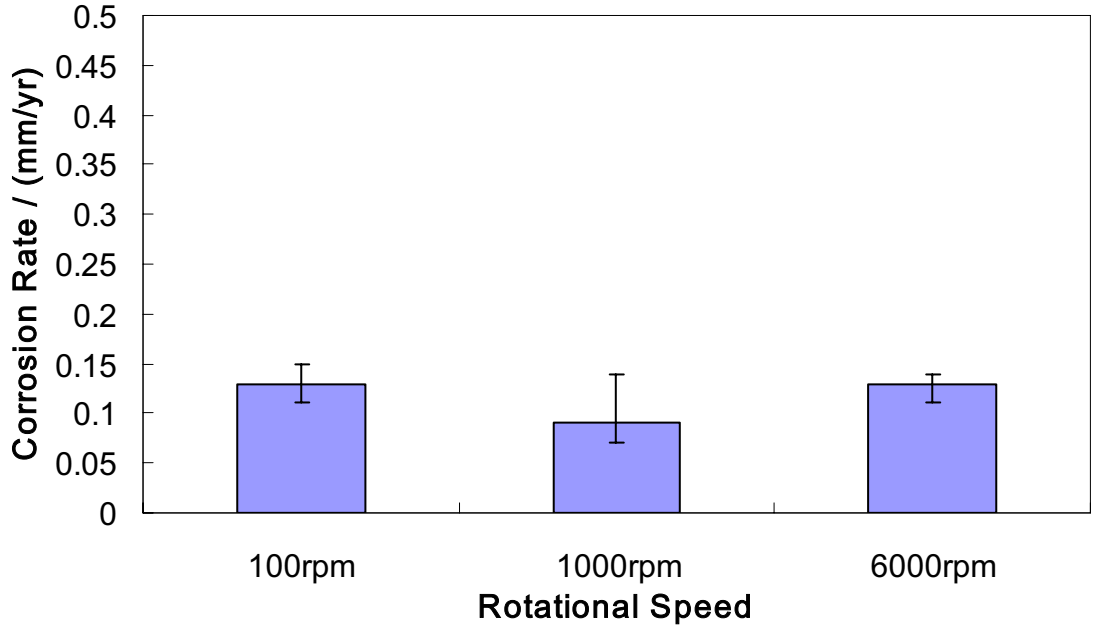

Figure 6. LPR corrosion rates for different rotational speeds at 5 ºC, pH4.0, 10% NaCl

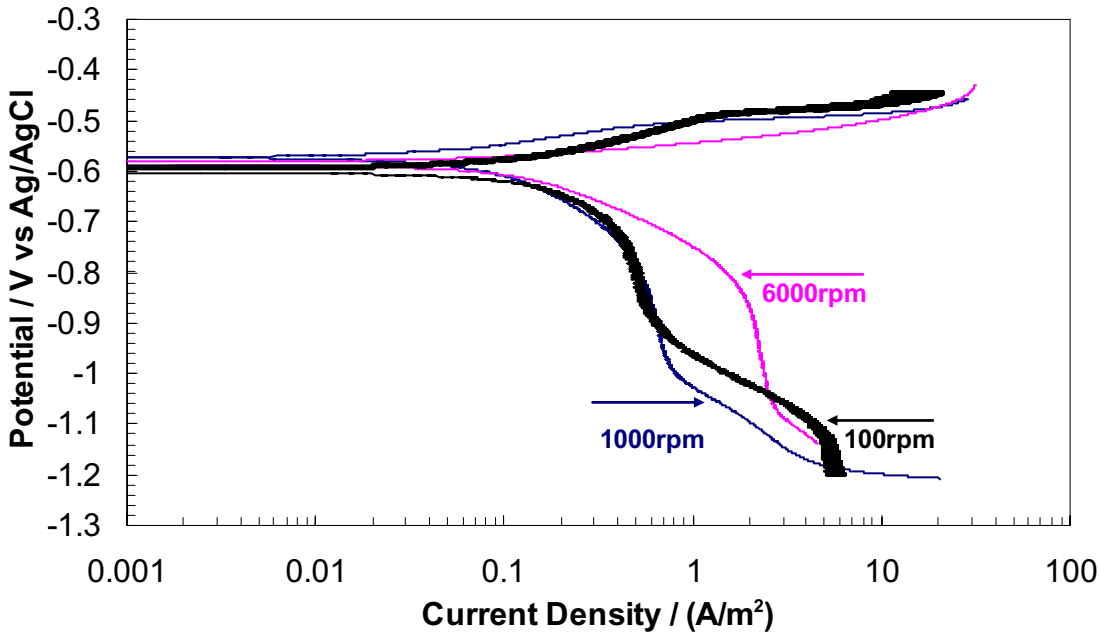

Figure 7. Potentiodynamic sweeps for different rotational speed (100, 1000, 6000rpm) at 5ºC, pH4.0, 10% NaCl

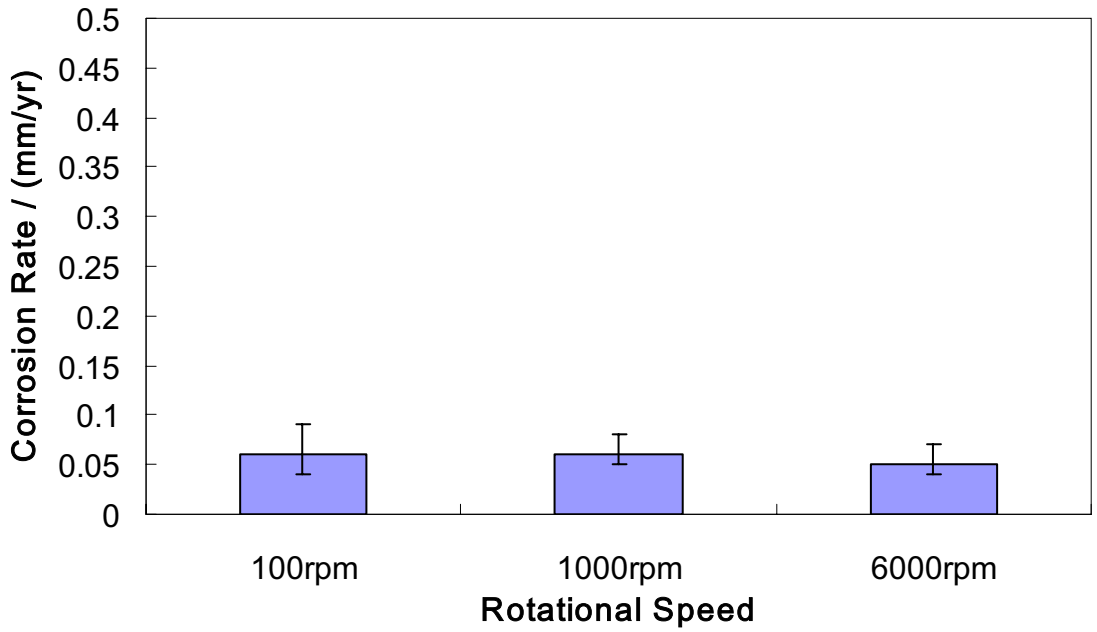

Figure 8. LPR corrosion rates for different rotational speeds at 5 ºC, pH4.0, 20% NaCl

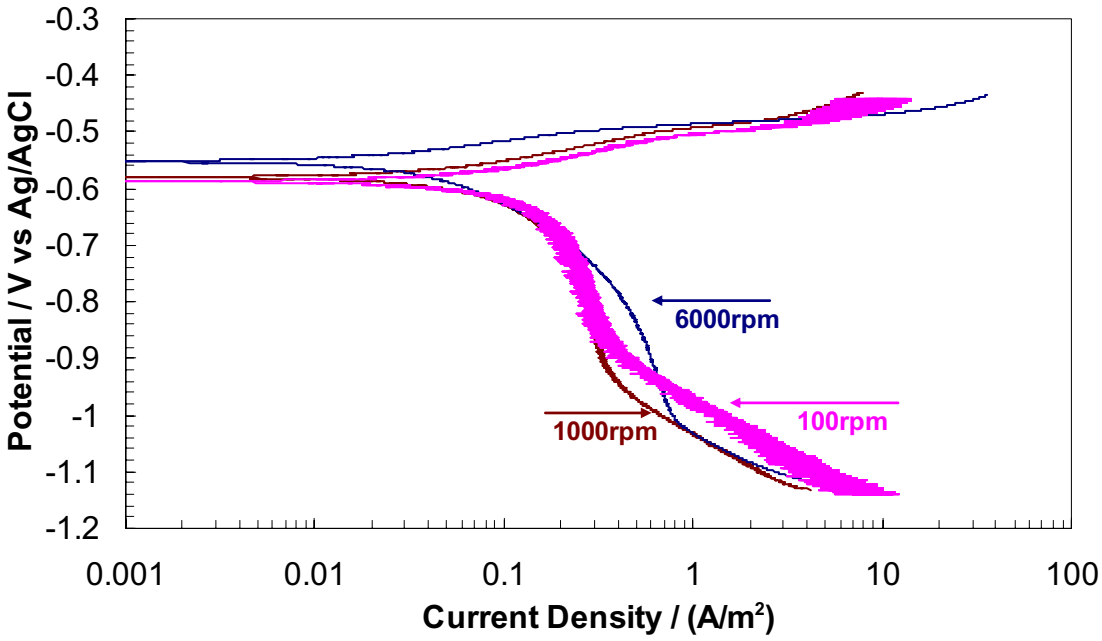

Figure 9. Potentiodynamic sweeps with different rotational speeds (100, 1000, 6000rpm) at 5ºC, pH4.0, 20% NaCl

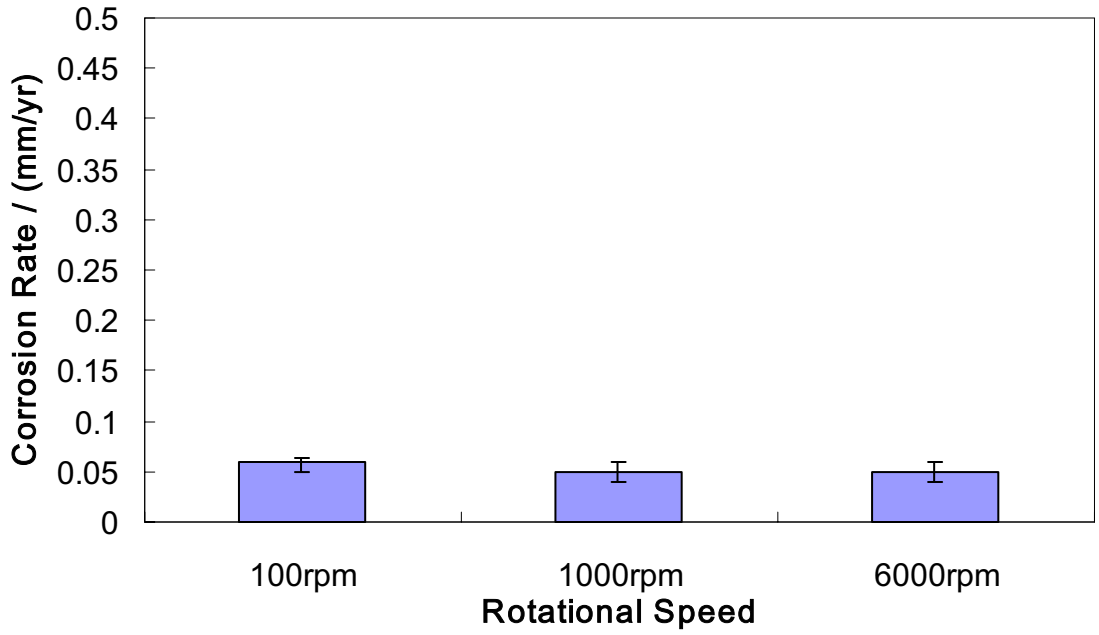

Figure 10. LPR corrosion rates at different rotational speeds at 5 ºC, pH4.0, 25% NaCl

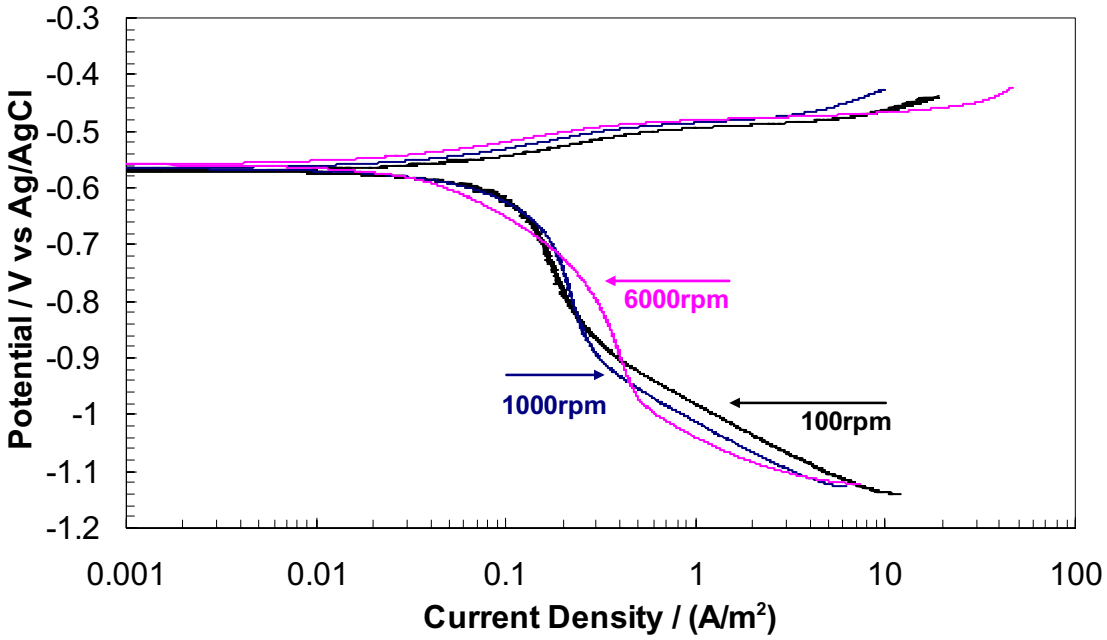

Figure 11. Potentiodynamic sweeps for different rotational speeds (100, 1000, 6000rpm) at 5ºC, pH4.0, 25% NaCl

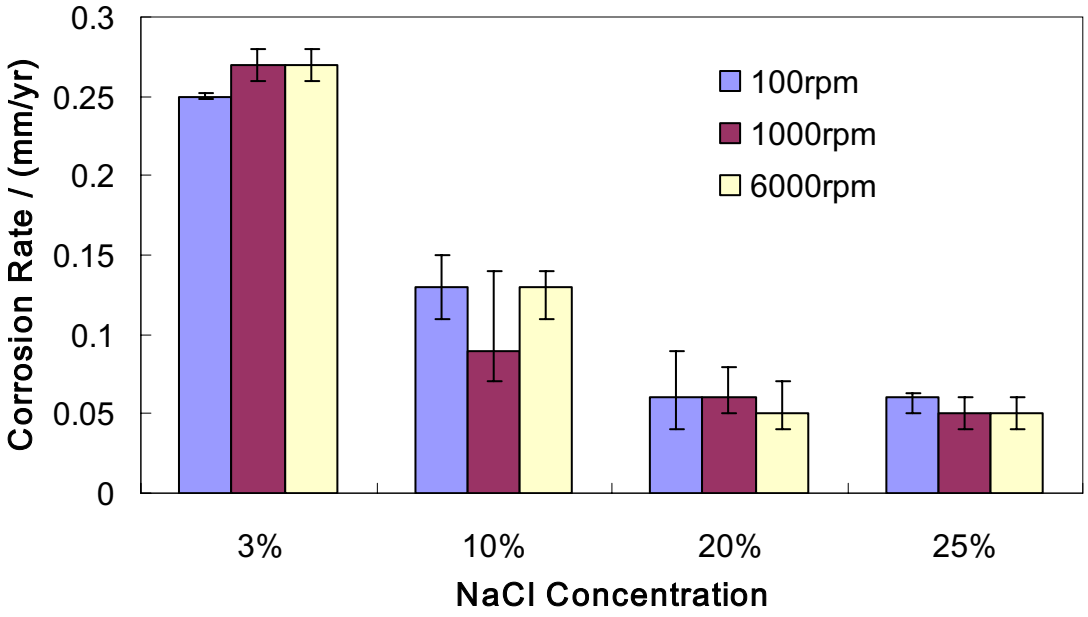

Figure 12. Comparison of LPR corrosion rates measured at 5 ºC, pH4.0, for 3 wt%, 10 wt%, 20 wt%, and 25 wt% NaCl at rotational speeds of 100, 1000, and 6000 rpm. 25% NaCl

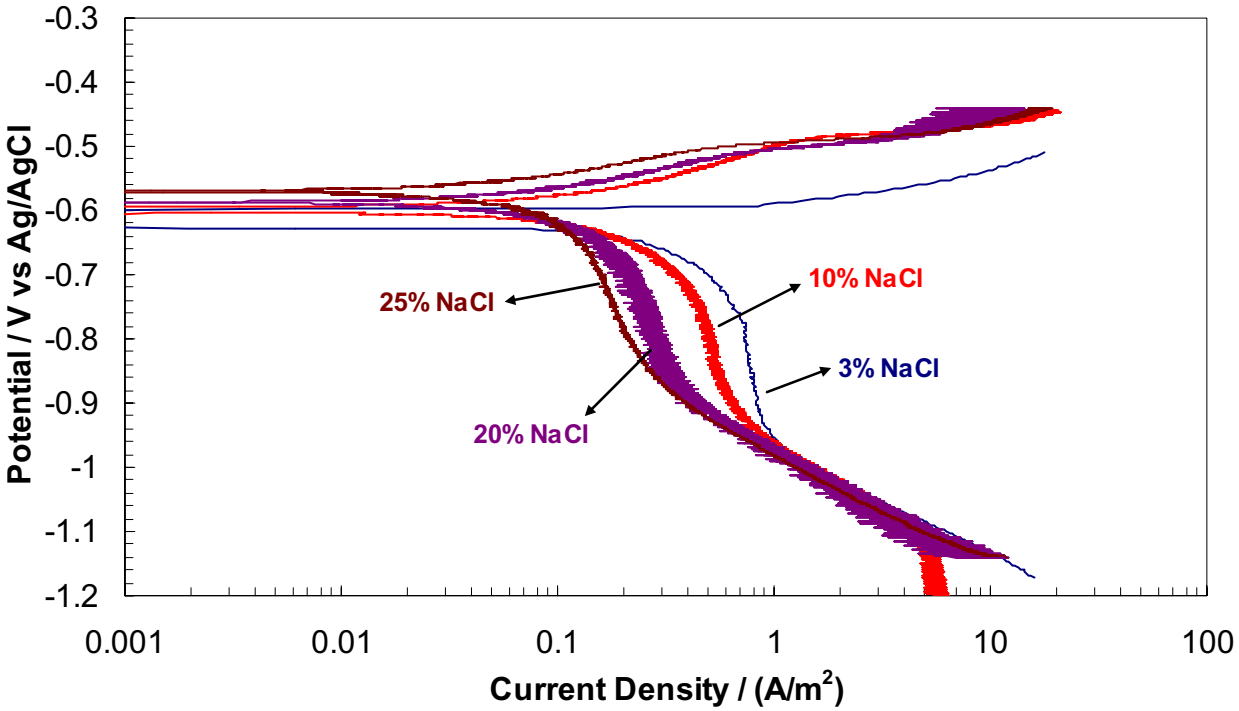

Figure 13. Potentiodynamic sweeps with different NaCl concentration (3%, 10%, 20%, 25%) at 5ºC pH4.0, 100rpm

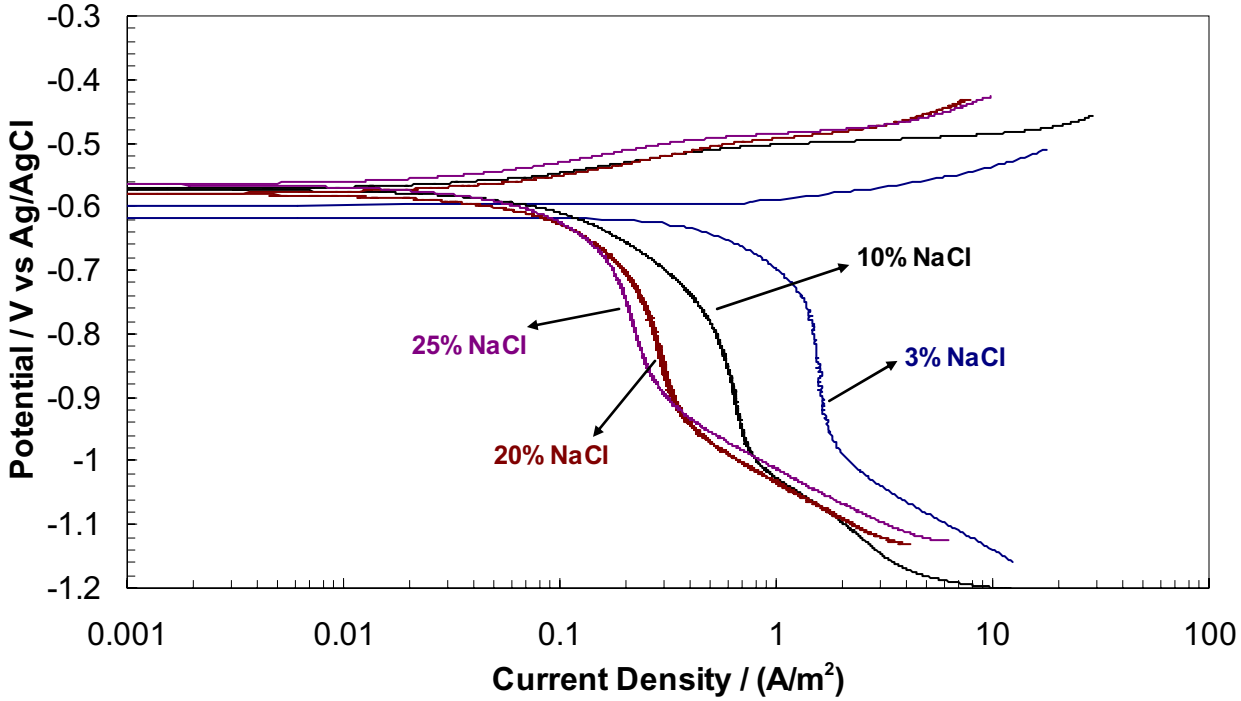

Figure 14. Potentiodynamic sweeps for different NaCl concentration (3%, 10%, 20%, 25%) at 5ºC, pH4.0, 1000rpm

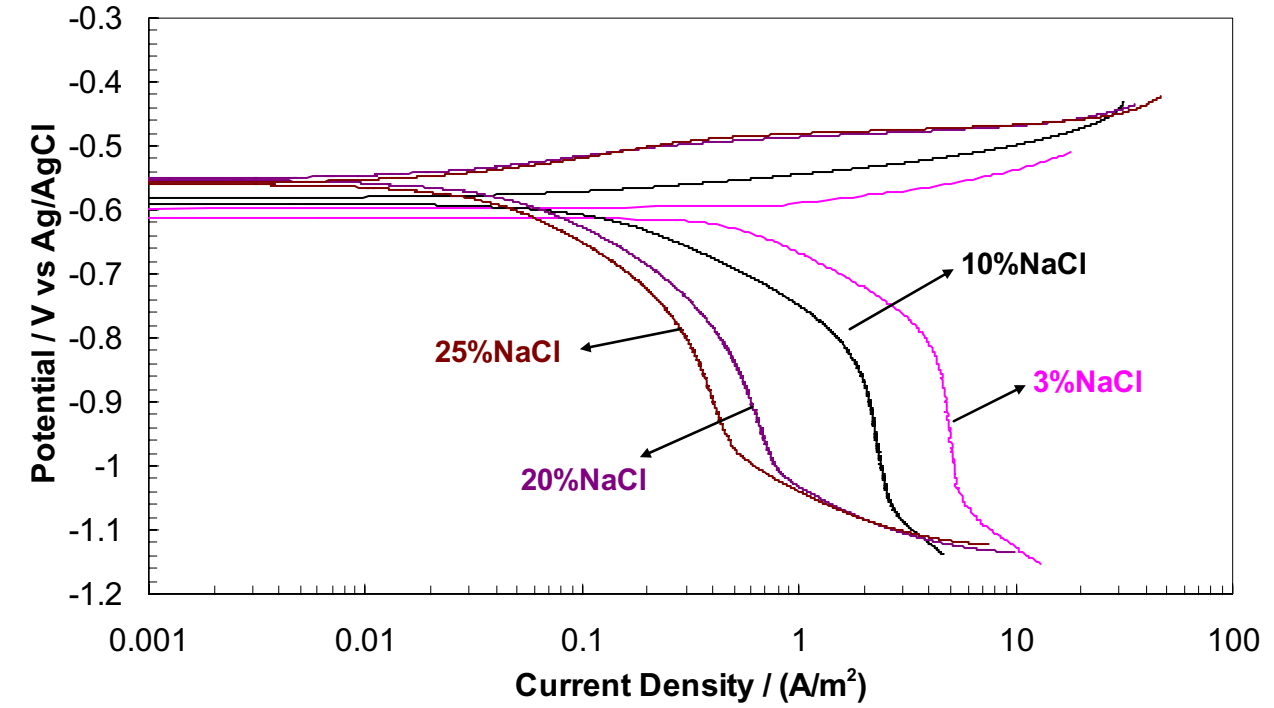

Figure 15. Potentiodynamic sweeps for different NaCl concentration (3%, 10%, 20%, 25%) at5ºC, pH4.0, 6000rpm